



Data Article

Electron spectroscopies of 3-hydroxyflavone and 7-hydroxyflavone in MCM-41 silica nanoparticles and in acetonitrile solutions. Experimental data and DFT/TD-DFT calculations



Anton Landström^a, Ari Paavo Seitsonen^{b,c,*}, Silvia Leccese^d, Hagop Abadian^d, Jean-François Lambert^d, Stefano Protti^{e,*}, Isabella Concina^{a,*}, Alberto Mezzetti^{d,*}

^a Division of Materials Science, Department of Engineering Sciences and Mathematics, Luleå Tekniska Universitet, Luleå, SE-971 87 Sweden

^b Département de Chimie, Ecole Normale Supérieure, 24 rue Lhomond, F-75005, Paris, France

^c Paris Sciences et Lettres Université, Sorbonne Université et Centre National du Recherche Scientifique (CNRS), F-75005, Paris, France

^d Laboratoire de Réactivité de Surface UMR CNRS 7197, Sorbonne Université, 4 place Jussieu, F-75005 Paris, France

^e PhotoGreen Lab, Department of Chemistry, University of Pavia, Viale Taramelli 10, I-27100, Pavia, Italy

ARTICLE INFO

Article history:

Received 11 October 2020

Revised 2 December 2020

Accepted 3 December 2020

Available online 8 December 2020

Keywords:

3-hydroxyflavone

7-hydroxyflavone

Excited-state intramolecular proton transfer

Florescent nanoparticles

MCM-41

Photostability of flavonoids

TD-DFT calculations on absorption and

fluorescence spectra of flavonoids

DOI of original article: [10.1016/j.dib.2020.108870](https://doi.org/10.1016/j.dib.2020.108870)

* Corresponding authors.

E-mail addresses: ari.p.seitsonen@iki.fi (A.P. Seitsonen), stefano.protti@unipv.it (S. Protti), isabella.concina@ltu.se (I. Concina), alberto.mezzetti@sorbonne-universite.fr (A. Mezzetti).

ABSTRACT

The data presented here concern the photophysical characterization of luminescent MCM-41 nanoparticles doped with 3-hydroxyflavone and 7-hydroxyflavone, two fluorescent flavonoids. UV-Vis and fluorescence spectra obtained on freshly-prepared samples and aged (2 months exposed to air) samples are shown. The effect of light exposure is also studied. In parallel, experiments have been carried out in acetonitrile solutions of the two flavonoids as a term of comparison. Time-dependent density functional theory calculations have also been used to simulate UV-Vis and emission spectra of different species for both flavonoids (neutral molecule, tautomers, cationic and anionic forms), taking into account the

effect of the surrounding medium (solvent). Density functional theory calculations of vibrational spectra (IR, Raman) of neutral and tautomeric species of 3HF and 7HF are also provided.

© 2020 Published by Elsevier Inc.

This is an open access article under the CC BY-NC-ND license (<http://creativecommons.org/licenses/by-nc-nd/4.0/>)

Specifications Table

Subject	Physical Chemistry
Specific subject area	Electronic spectroscopy, photophysics
Type of data	Spectra Tables
How data were acquired	UV-Vis spectra were recorded with an Agilent Cary5000 spectrophotometer. An integrating sphere was used to record reflectance. Spectra were reconstructed through Kubelka-Munk transform. Steady-state photoluminescence spectra of flavonoids in silica NPs were recorded with Edinburgh instruments FLS980 spectrofluorimeter (excitation source: Xenon arc lamp). Photobleaching tests were performed by doing repeated emission scans of the samples in 3-minute intervals. The computer codes ORCA [1] and Gaussian09 Revision A.02 [2] were used in DFT and TD-DFT calculations.
Data format	Raw
Parameters for data collection	UV-Vis and fluorescence spectra of 3HF and 7HF in different environments and under different conditions (air exposure, UV exposure). Simulation of UV-Vis and fluorescence spectra (by TD-DFT calculations) of 3HF and 7HF in gas phase and acetonitrile (MeCN).
Description of data collection	UV-Vis and fluorescence spectra from 3-hydroxyflavone (3HF) and 7-hydroxyflavone (7HF) embedded in MCM-41 silica nanoparticles before and after 2 months of exposure to air at 298 K Evolution of fluorescence spectra of 3HF and 7HF in MCM-41 matrices and in Acetonitrile (MeCN) solutions under UV irradiation Simulation via TD-DFT calculations of absorption and fluorescence spectra of neutral, anionic, cationic, tautomeric forms of 3HF and 7HF in gas phase and in MeCN Simulation via DFT calculations of most intense IR and Raman bands of neutral and tautomeric form of 3HF and neutral and tautomeric form of 7HF, in gas phase and in MeCN
Data accessibility	With the article
Related research article	Landström A, Leccese S, Abadian H, Lambert J-F, Concina I, Protti S, Ari Paavo Seitsonen AP, Mezzetti A, "Fluorescent silica MCM-41 nanoparticles based on flavonoids: Direct post-doping encapsulation and spectral characterization. <i>Dyes and Pigments</i> 185 (2021) 108870, for a co-submission research article. https://doi.org/10.1016/j.dyepig.2020.108870

Value of the Data

- UV-Vis and fluorescence spectra of 3HF and 7HF in MCM-41 silica nanoparticles (NPs) remain fluorescent after 2 month of air exposure at room temperature. In the case of 7HF silica NPs, the fluorescence spectrum is modified compared to the spectrum of freshly-prepared 7HF silica NPs.
- Fluorescence spectra recorded at different time of UV irradiation show the effect of photodecomposition in the emission properties of MCM-41 flavonoid-doped NPs and of flavonoid solutions in MeCN.
- TD-DFT calculations of UV-Vis and fluorescence spectra (in vacuum and in MeCN) of 3HF and 7HF both in neutral, tautomeric, anionic, cationic forms are reported. They can be useful in

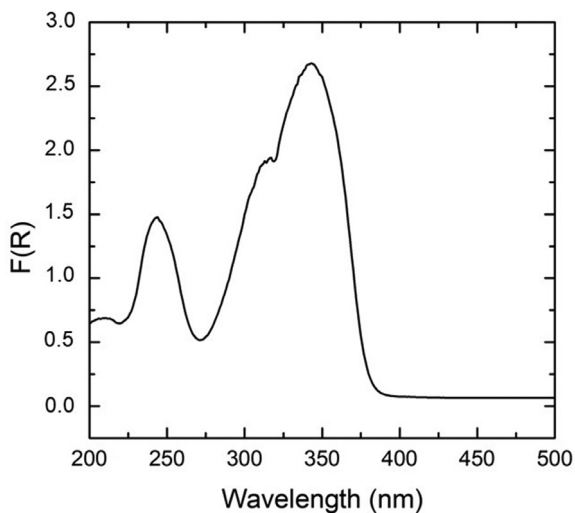


Fig. 1. F(R) spectrum (approximately equivalent to UV-Vis absorbance spectrum) of aged (2 months of air exposure at 298K) 3HF-doped MCM-41 NPs. F(R) spectrum of freshly-prepared 3HF-doped MCM-41 NPs is shown in Fig. 3 of the related research paper [6]. F(R) is the Kubelka-Munk transform of the reflectance R, $F(R) = (1-R)^2/2R$.

the interpretation of experimental absorption and fluorescence spectra of 3HF and 7HF and in the assessment of environmental effects on these spectra.

- TD-DFT simulation of electronic spectra and DFT simulation of vibrational spectra of 3HF and 7HF in vacuum and in MeCN can be useful in the interpretation of experimental FTIR and Raman spectra of 3HF and 7HF and in the assessment of environmental effects on these spectra.

1. Data Description

3HF and 7HF are fluorescent molecules widely used in biophysics and analytical chemistry [3–5]. In this work and in the related research article [6] the fluorescence properties of these two flavonoids inside MCM-41 silica NPs have been studied. The spectra presented here focus first on the effect of air exposure on the emission properties of the NPs. Figs. 1 and 2 show the UV-Vis spectra after 2 months of air exposure. Only minimal changes are observed compared to the spectra recorded on freshly-prepared NPs (reported in [6]). In Figs. 3 and 4 the emission spectra of aged flavonoid-doped NPs are reported. These two figures show that both kind of NPs remain fluorescent. For 3HF-doped aged NPs a slight attenuation of the fluorescent intensity is observed compared to freshly-prepared 3HF-doped NPs [6], without almost any modification of the spectral shape. For 7HF-doped NPs, 2 months of air exposure modify quite strongly the shape of the emission spectra.

Figs. 5 and 6 show the effect of UV irradiation exposure of the fluorescent properties of the two kinds of flavonoid-doped NPs. For a comparison, Figs. 7 and 8 show the same kind of experiment for 3HF and 7HF in MeCN solutions. Fig. 8 shows that for 7HF in MeCN UV exposure lead to an increase of emission at ~ 375 nm.

Table 1 reports the results of TD-DFT calculations used to simulate absorption and fluorescence spectra of 3HF and 7HF in different forms (neutral, tautomeric, anionic, cationic). The results obtained in gas phase and in MeCN are compared.

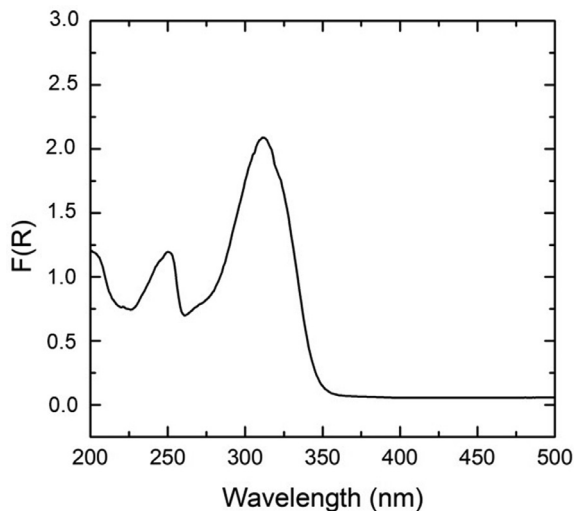


Fig. 2. F(R) spectrum (approximately equivalent to UV-Vis absorbance spectrum) of aged (2 months of air exposure at 298K) 7HF-doped MCM-41 NPs. UV-Vis spectrum of freshly-prepared 7HF-doped MCM-41 NPs is shown in Fig. 3 of the related research paper [6]. F(R) is the Kubelka-Munk transform of the reflectance R, $F(R) = (1-R)^2/2R$.

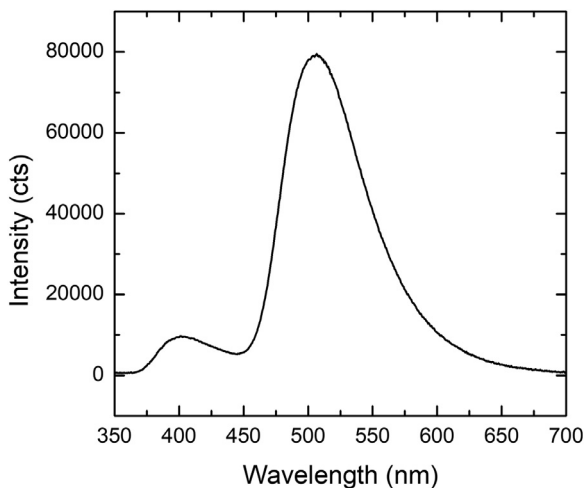


Fig. 3. Fluorescence spectrum ($\lambda_{exc} = 320$ nm) of aged (2 months of air exposure at 298K) 3HF-doped MCM-41 NPs. The fluorescence spectrum of freshly-prepared 3HF-doped MCM-41 NPs is shown in Fig. 3 of the related research paper [6].

Table 2 contains the most intense bands in the computed IR and Raman spectra of 3HF and 7HF in neutral and tautomeric forms; also in this case results obtained in gas phase and in MeCN are compared.

Fig. 9 helps to better understand data reported in Tables 1 and 2.

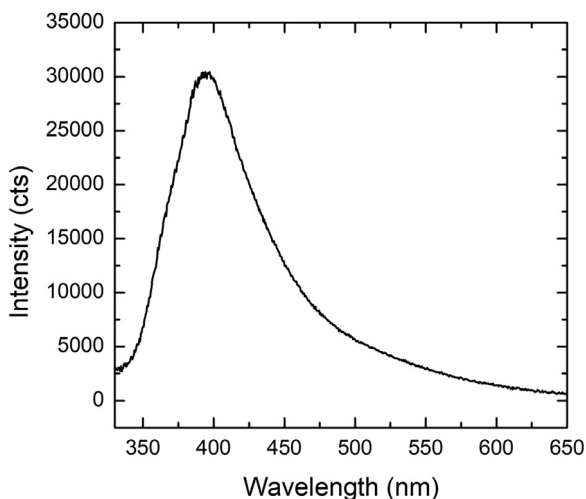


Fig. 4. Fluorescence spectrum ($\lambda_{\text{exc}} = 300$ nm) of aged (2 months of air exposure at 298K) 7HF-doped MCM-41 NPs. The fluorescence spectrum of freshly-prepared 7HF-doped MCM-41 NPs is shown in Fig. 3 of the related research paper [6].

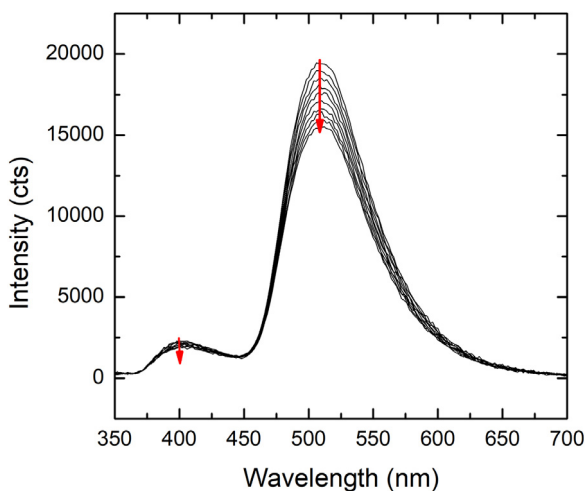


Fig. 5. Fluorescence spectra ($\lambda_{\text{exc}} = 320$ nm) of freshly-prepared 3HF-doped MCM-41 NPs after different period of UV light ($\lambda = 320$ nm) exposure. Spectra were recorded every 3 minutes. Intensity (for both emission bands) decreases with time, as indicated by the red arrows.

2. Experimental Design, Materials and Methods

Chemicals. 3HF and 7HF were purchased from Sigma-Aldrich and recrystallized from cyclohexane. Acetonitrile (MeCN) for post-doping procedure was of spectroscopic grade. Fluorescence analysis were carried out using anhydrous MeCN.

Synthesis of silica NPs. MCM-41 NPs were prepared by following the protocol of Ref. [7]. An aqueous solution of cetyltrimethylammonium bromide (CTAB), mixed with aqueous ammonia was left under stirring at a constant temperature of 35 °C. Then tetraethyl orthosilicate (TEOS) was added. The TEOS/CTAB/ NH_4OH mixture was left at 35 °C for 2 h. Then, the system was transferred to a tightly sealed Teflon bottle placed in a drying oven at 100 °C and left under

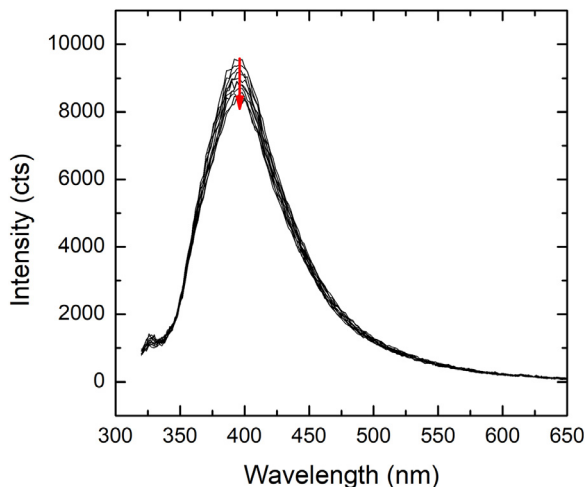


Fig. 6. Fluorescence spectra ($\lambda_{\text{exc}} = 300$ nm) of freshly-prepared 7HF-doped MCM41 NPs after different period of UV light ($\lambda = 300$ nm) exposure. Spectra were recorded every 3 minutes. Intensity decreases with time, as indicated by the red arrow.

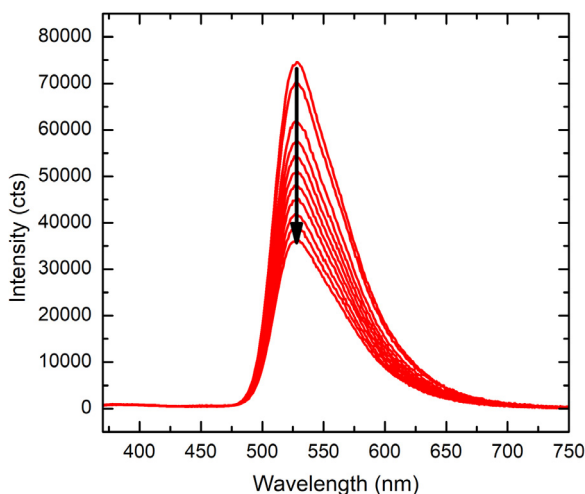


Fig. 7. Fluorescence spectra ($\lambda_{\text{exc}} = 320$ nm) of 3HF in a MeCN solution after different period of UV light ($\lambda = 320$ nm) exposure. Intensity decreases with UV exposure time, as shown by the black arrow. Spectra were recorded every 3 minutes.

autogenous pressure overnight. After filtration, the final step was the removal of CTAB within the pores of the MCM-41 by calcination: the solid sample was placed in a crucible in a programmable calcination oven under ambient air and the temperature was increased from 20 to 300 °C in 2 ½ h. Then the temperature was kept constant at 300 °C for 2 h. Subsequently, temperature was increased from 300 to 550 °C in 2 h. Then the temperature was kept constant at 550 °C for 12 h.

Preparation of flavonoid-doped NPs MCM-41 NPs were added to 10^{-3} M MeCN solutions of 3HF and 7HF. Samples were stirred for 5 min, centrifuged for 45 min at 4000 rpm to separate the solid (containing MCM-41 matrix with the flavonoids encapsulated). The solid was then exposed to air for 48 h in a Petri dish to let the solvent evaporate.

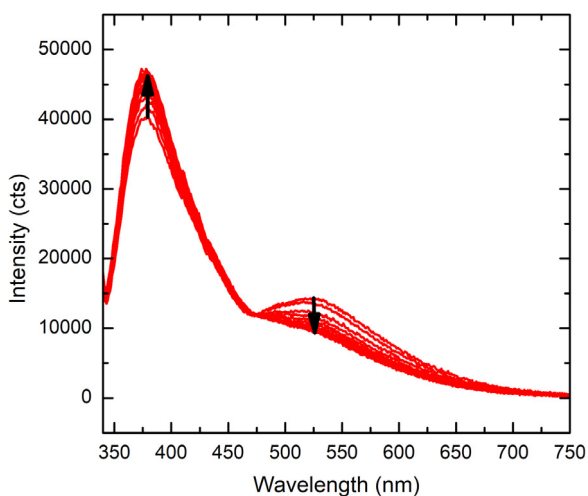


Fig. 8. Fluorescence spectra ($\lambda_{\text{exc}} = 300$ nm) of 7HF in an aerated MeCN solution after different period of UV light ($\lambda = 300$ nm) exposure. Spectra were recorded every 3 minutes. The ~ 525 nm band decreases its intensity with exposure time, the ~ 375 nm band increases its intensity with exposure time, as shown by the black arrows.

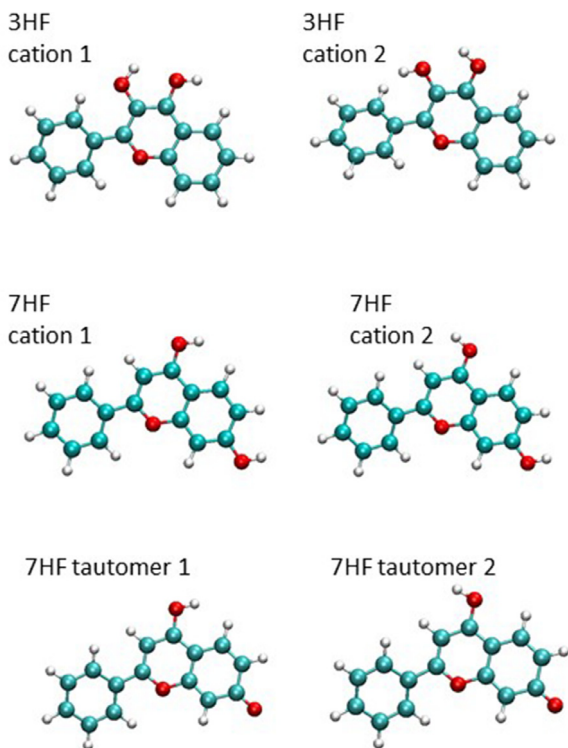


Fig. 9. The structure of the species mentioned in Tables 1 and 2 that exist in two forms.

Table 1

energy of the absorption and fluorescence spectra of the different species in gas phase and in acetonitrile. Energy is first given in eV, then in nm. For absorbance transitions, the third row indicates the intensity.

3HF neutral										
free/gas phase										
Absorbance (eV)	3.55	3.99	4.19	4.35	4.56	4.77	4.92	4.99	5.21	5.29
(nm)	349	310	296	285	272	260	252	248	238	234
Intensity	0.375	0.0	0.142	0.026	0.010	0.079	0.074	0.072	0.0	0.095
Fluorescence (eV)	3.1278									
(nm)	396.39									
in MeCN										
Absorbance (eV)	3.50	4.09	4.12	4.33	4.58	4.79	4.91	5.03	5.24	5.27
(nm)	355	303	301	287	271	259	252	247	237	235
Intensity	0.488	0.125	0.071	0.024	0.001	0.149	0.064	0.111	0.065	0.004
Fluorescence (eV)	2.9078									
(nm)	426.38									
3HF tautomer										
free/gas phase										
Absorbance (eV)	2.57	3.25	3.77	3.81	4.06	4.17	4.46	4.54	4.57	4.86
(nm)	482	381	329	325	305	297	278	273	272	255
Intensity	0.355	0.0	0.002	0.059	0.118	0.055	0.049	0.0	0.038	0.0
Fluorescence (eV)	2.29									
(nm)	540									
in MeCN										
Absorbance (eV)	2.61	3.46	3.76	3.86	4.24	4.29	4.52	4.53	4.71	4.90
(nm)	476	358	330	321	293	289	274	274	263	253
Intensity	0.458	0.0	0.106	0.036	0.077	0.037	0.129	0.008	0.001	0.295
Fluorescence (eV)	2.18									
(nm)	568									
3HF anion										
free/gas phase										
Absorbance (eV)	2.33	2.56	2.65	2.67	2.94	3.12	3.18	3.29	3.43	3.56
(nm)	531	484.19	467	465	421	397	389	377	361	348
Intensity	0.218	0.000	0.001	0.0	0.0	0.001	0.108	0.001	0.067	0.001
Fluorescence (eV)	2.03									
(nm)	611									
in MeCN										
Absorbance (eV)	2.60	3.11	3.66	3.85	3.87	3.90	3.95	4.20	4.21	4.30
(nm)	477	399	339	322	320	318	314	295	295	288
Intensity	0.374	0.0	0.031	0.088	0.002	0.062	0.0	0.041	0.196	0.004
Fluorescence (eV)	2.18									
(nm)	568									
3HF cation 1										
free/gas phase										
Absorbance (eV)	3.13	3.20	3.61	4.42	4.76	4.88	4.90	5.02	5.14	5.52
(nm)	397	387	343	281	261	254	253	247	241	225
Intensity	0.104	0.509	0.039	0.005	0.013	0.056	0.148	0.055	0.0	0.004
Fluorescence (eV)	2.39									
(nm)	519									

(continued on next page)

Table 1 (continued)

in MeCN										
Absorbance (eV)	3.17	3.48	3.59	4.49	4.75	4.97	5.10	5.13	5.40	5.47
(nm)	391	356	345	276	261	249	243	242	230	227
Intensity	0.665	0.002	0.114	0.014	0.025	0.243	0.142	0.079	0.0	0.263
Fluorescence (eV)	2.7558									
(nm)	449.9									
3HF cation 2 free/gas phase										
Absorbance (eV)	3.34	3.50	3.59	4.42	4.79	5.06	5.13	5.23	5.60	5.65
(nm)	371	355	346	280	259	245	242	237	221	219
Intensity	0.398	0.007	0.115	0.023	0.020	0.118	0.019	0.313	0.034	0.083
Fluorescence (eV)	2.8227									
(nm)	439.23									
in MeCN										
Absorbance (eV)	3.33	3.62	3.68	4.48	4.78	5.07	5.17	5.19	5.59	5.61
(nm)	372	342	337	277	260	244	240	239	222	221
Intensity	0.529	0.079	0.057	0.031	0.031	0.164	0.063	0.351	0.074	0.066
Fluorescence (eV)	2.82									
(nm)	440									
7HF neutral free/gas phase										
Absorbance (eV)	3.53	4.11	4.19	4.61	4.67	4.76	4.96	5.21	5.23	5.28
(nm)	351	302	296	269	265	261	251	238	237	235
Intensity	0.001	0.305	0.079	0.216	0.035	0.0	0.050	0.003	0.009	0.086
Fluorescence (eV)	2.85									
(nm)	436									
in MeCN										
Absorbance (eV)	3.78	3.95	4.18	4.46	4.53	5.00	5.08	5.16	5.33	5.36
(nm)	328	314	297	278	273	248	244	240	233	231
Intensity	0.009	0.474	0.111	0.243	0.027	0.074	0.007	0.037	0.017	0.159
Fluorescence (eV)	3.28									
(nm)	378									
7HF tautomer 1 free/gas phase										
Absorbance (eV)	2.65	2.77	3.86	4.08	4.10	4.18	4.36	4.45	4.59	4.76
(nm)	467	448	321	304	302	297	284	279	270	261
Intensity	0.232	0.0	0.010	0.014	0.406	0.084	0.001	0.006	0.038	0.005
Fluorescence (eV)	1.74									
(nm)	713									
in MeCN										
Absorbance (eV)	2.86	3.37	4.02	4.10	4.23	4.57	4.67	4.67	4.83	4.93
(nm)	434	368	309	303	293	271	266	265	256	252
Intensity	0.406	0.0	0.154	0.333	0.007	0.083	0.042	0.003	0.281	0.021
Fluorescence (eV)	2.09									
(nm)	594									

(continued on next page)

Table 1 (continued)

7HF tautomer 2										
free/gas phase										
Absorbance (eV)	2.59	2.70	3.75	3.98	3.99	4.07	4.14	4.50	4.65	4.66
(nm)	479	459	331	312	310	304	299	275.59	267	266
Intensity	0.215	0.0	0.015	0.008	0.134	0.039	0.330	0.008	0.080	0.002
Fluorescence (eV)	1.68									
(nm)	738									
in MeCN										
Absorbance (eV)	2.74	3.25	3.89	4.05	4.20	4.49	4.56	4.63	4.79	4.86
(nm)	452	382	319	306	295	276	272	268	259	255
Intensity	0.365	0.0	0.149	0.399	0.008	0.081	0.0	0.067	0.252	0.029
Fluorescence (eV)	2.03									
(nm)	610									
7HF anion										
free/gas phase										
Absorbance (eV)	2.05	2.64	2.73	2.74	3.05	3.23	3.29	3.38	3.45	3.56
(nm)	605	470	454	452	406	383	377	367	359	348
Intensity	0.091	0.0	0.007	0.0	0.0	0.0	0.0	0.005	0.0	0.0
Fluorescence (eV)	1.50									
(nm)	829									
in MeCN										
Absorbance (eV)	2.89	3.70	3.86	3.95	4.08	4.31	4.36	4.46	4.63	4.68
(nm)	429	335	321	314	304	288	285	278	268	265
Intensity	0.193	0.0	0.003	0.032	0.020	0.278	0.017	0.366	0.306	0.012
Fluorescence (eV)	2.19									
(nm)	565									
7HF cation 1										
free/gas phase										
Absorbance (eV)	3.35	3.42	3.82	4.31	4.81	4.85	5.02	5.33	5.44	5.51
(nm)	370	363	325	288	258	256	247	233	228	225
Intensity	0.587	0.014	0.063	0.031	0.107	0.092	0.078	0.059	0.191	0.003
Fluorescence (eV)	3.00									
(nm)	413									
in MeCN										
Absorbance (eV)	3.35	3.72	3.84	4.29	4.92	5.07	5.10	5.36	5.45	5.70
(nm)	370	334	323	289	252	244	243	231	228	217
Intensity	0.653	0.017	0.119	0.083	0.178	0.206	0.038	0.041	0.173	0.133
Fluorescence (eV)	2.94									
(nm)	421									
7HF cation 2										
free/gas phase										
Absorbance (eV)	3.33	3.49	3.75	4.24	4.83	4.92	5.08	5.33	5.48	5.58
(nm)	372	355	330	292	256	252	244	232	226	222
Intensity	0.496	0.012	0.144	0.040	0.140	0.050	0.16	0.071	0.114	0.009
Fluorescence (eV)	2.74									
(nm)	453									

(continued on next page)

Table 1 (continued)

	in MeCN									
Absorbance (eV)	3.34	3.73	3.82	4.27	4.93	5.08	5.13	5.38	5.47	5.70
(nm)	371	332	325	290	252	244	242	231	227	217
Intensity	0.607	0.037	0.138	0.094	0.169	0.248	0.019	0.042		
	0.148	0.117								
Fluorescence (eV)	2.89									
(nm)	428									

Table 2

Main IR and Raman bands for 3HF and 7HF in the neutral and tautomeric forms. First column, energy in cm^{-1} ; second column, IR relative intensity; third column, Raman relative intensity.

3HF neutral free/gas phase					
373	22	—	1375	84	—
678	50	—	1441	202	—
708	41	—	1504	87	—
778	75	—	1513	44	—
1014	—	162	1532	31	—
1110	37	—	1604	31	441
1156	98	—	1640	35	1569
1210	74	—	1649	124	368
1226	56	—	1656	178	321
1323	65	—	1684	138	186
1337	26	175	3187	26	324
1356	211	197	3201	—	283
1370	33	—	3522	154	174
in MeCN					
590	161	—	1504	126	—
778	108	—	1513	106	—
1011	—	512	1604	521	3231
1156	275	—	1640	706	1915
1210	75	446	1649	—	2597
1226	283	—	1656	109	—
1323	281	—	1684	—	3006
1337	238	—	3187	—	622
1356	—	1543	3201	—	834
1441	391	675	3522	288	439
3HF tautomer free/gas phase					
904	78	—	1527	69	221
1012	—	289	1558	—	969
1177	—	252	1585	134	216
1211	—	258	1619	140	—
1257	—	371	1637	—	1504
1264	72	—	1652	—	844
1324	83	—	3150	97	243
1385	88	—	3173	—	168
1417	78	1595	3186	—	344
1446	490	762	3187	—	253
1519	227	—	3205	—	292
in MeCN					
788	95	—	1483	180	—
856	96	—	1519	352	—
1004	—	1031	1527	185	—

(continued on next page)

Table 2 (continued)

1137	119	—	1558	322	7067
1211	—	1287	1585	172	1839
1257	368	1584	1619	129	—
1324	355	—	1637	—	7547
1385	532	—	1652	—	3714
1417	—	1838	3221	274	—
1446	840	10211	—	—	—
7HF neutral					
free/gas phase					
369	97	—	1663	286	330
1020	—	86	1710	434	241
1158	101	—	3157	—	164
1168	166	—	3175	—	134
1253	—	105	3186	—	169
1270	—	267	3195	—	163
1318	143	—	3195	—	101
1390	321	140	3208	—	71
1487	195	—	3209	—	84
1606	46	263	3221	—	91
1644	—	550	3811	102	197
1651	96	386	—	—	—
in MeCN					
612	132	—	1644	741	626
1110	96	—	1651	—	2862
1158	166	—	1663	942	2339
1168	271	—	1710	370	—
1253	—	308	3165	—	317
1270	—	1245	3175	—	313
1284	116	—	3186	—	370
1318	273	—	3195	—	539
1378	118	—	3208	—	298
1390	566	589	3209	—	326
1484	136	—	3221	—	301
1487	250	—	3811	240	403
1606	161	1455	—	—	—
7HF tautomer 1					
free/gas phase					
1152	78	—	1611	112	—
1201	187	—	1626	78	804
1469	163	583	1643	—	781
1568	312	3940	1680	207	—
1586	515	776	1683	502	—
in MeCN					
1201	295	592	1626	—	590
1244	—	716	1643	—	1133
1469	525	1358	1680	305	477
1568	352	585	1683	776	—
1586	1545	4530	3188	—	550
1611	395	3487	—	—	—
7HF tautomer 2					
free/gas phase					
359	84	---	1564	401	6339
779	63	---	1587	291	---
1142	97	---	1642	---	869
1276	192	---	1682	616	---
1426	79	---	1691	98	---
1463	80	---	3812	68	---

(continued on next page)

Table 2 (continued)

in MeCN					
741	157	---	1587	1372	7828
881	160	---	1615	194	1825
1013	264	---	1642	---	1307
1142	340	---	1682	295	---
1242	137	923	1691	578	---
1276	373	---	3176	207	---
1426	161	---	3193	205	---
1463	418	988	3202	633	---
1564	368	---	3812	141	---

UV-Vis spectra of flavonoid-doped NPs were recorded with an Agilent Cary5000 spectrophotometer. An integrating sphere was used to record reflectance; spectra were obtained through Kubelka-Munk transform.

Steady-state photoluminescence spectra of flavonoid-doped NPs were recorded with Edinburgh instruments FLS980 spectrofluorimeter. A Xenon arc lamp was used as excitation source. Photobleaching tests were performed by doing repeated emission scans of the samples in 3-minutes intervals.

UV-Vis absorption spectra in MeCN solutions were carried out on a Jasco V-550 spectrophotometer or on a Agilent Cary 5000 spectrophotometer. Fluorescence spectra of MeCN solution were carried out on a Perkin Elmer LS-55 spectrofluorometer or on an Edinburgh instruments FLS980 spectrofluorimeter. Photobleaching tests were performed by doing repeated emission scans of the samples in 3-minute intervals.

Theoretical calculations. Density functional theory (DFT) [8] and time-dependent DFT [9] calculations were carried out on both flavonoids in different states (neutral, tautomer, anion, cation). DFT was used to calculate the ground-state S_0 geometries and vibrational spectra; TD-DFT for absorption and fluorescence spectra, the latter in the first singlet state S_1 . We employed the B3LYP [10] as the approximation in the exchange-correlation functional. The basis set cc-pVTZ in the calculation of the vibrational spectra and aug-cc-pVTZ in the calculations of TDDFT were used unless otherwise mentioned. The calculations have been performed with a free-standing molecule and using implicit solvation within the conductor-like polarisable continuum model (CPCM) [11] for MeCN.

The computer codes ORCA [1] and Gaussian09 Revision A.02 [2] were employed. We applied large integration grids and strict convergence criteria, "Grid5" and "tight SCF" in the input of ORCA and "Integral(UltraFine)" in the input of G09.

Declaration of Competing Interest

The authors declare that they have no known competing financial interests or personal relationships which have, or could be perceived to have, influenced the work reported in this article.

Acknowledgements

The authors acknowledge the financial support from Knut & Alice Wallenberg foundation, Luleå University of Technology laboratory fund program, and Kempe foundation for partial funding. I.C. acknowledges VINNOVA under the VINNMER Marie Curie incoming Grant for partial funding (project "Light Energy", LiEN, 2015-01513). A.M. and S.L. acknowledge partial funding from the Labex Matisse "instrumentation" program.

Supplementary Materials

Supplementary material associated with this article can be found in the online version at doi:[10.1016/j.dib.2020.106630](https://doi.org/10.1016/j.dib.2020.106630).

References

- [1] F Neese, Software update: the ORCA program system, version 4.0 (WIREs, Comput Mol Sci 8 (2018) e1327, doi:[10.1002/wcms.1327](https://doi.org/10.1002/wcms.1327)).
- [2] M. J. Frisch et alia, Gaussian, Inc., Wallingford CT, 2009
- [3] S Protti, A Mezzetti, Any colour you like. Excited state and ground state proton transfer in flavonols and applications, in: A Albini (Ed.), Specialistic Periodical Report: Photochemistry, 40, Royal Society of Chemistry, 2012, pp. 295–322, doi:[10.1039/9781849734882-00295](https://doi.org/10.1039/9781849734882-00295).
- [4] A Mezzetti, S Protti, Flavonols and 3-hydroxychromones: new applications for a class of environment-sensitive fluorescent molecules, *Chimica Oggi – Chem. Today* 38 (2020) 34–37.
- [5] IE Serdiuk, AS Varenikov, AD Roshal, 7-hydroxyflavone revisited: spectral, acid-base properties, and interplay of the protolytic forms in the ground and excited states, *J. Phys. Chem. A* 118 (2014) 3068–3080, doi:[10.1021/jp412334x](https://doi.org/10.1021/jp412334x).
- [6] A Landström, S Leccese, H Abadian, J-F. Lambert, I Concina, S Protti, AP Ari Paavo Seitsonen, A Mezzetti, Fluorescent silica MCM-41 nanoparticles based on flavonoids: Direct post-doping encapsulation and spectral characterization, *Dyes and Pigments* 185 (2021) 108870, doi:[10.1016/j.dyepig.2020.108870](https://doi.org/10.1016/j.dyepig.2020.108870).
- [7] V Meynen, P Cool, EF Vansant, Verified syntheses of mesoporous materials, *Micropor. Mesoporous Mater.* 125 (2019) 170–223, doi:[10.1016/j.micromeso.2009.03.046](https://doi.org/10.1016/j.micromeso.2009.03.046).
- [8] P Hohenberg, W Kohn, Inhomogenous electron gas, *Phys. Rev. B* 136 (1964) 864–871, doi:[10.1103/PhysRev.136.B864](https://doi.org/10.1103/PhysRev.136.B864).
- [9] E Runge, EKU Gross, Density-functional theory for time-dependent systems, *Phys. Rev. Lett.* 52 (1984) 997–1000, doi:[10.1103/PhysRevLett.52.997](https://doi.org/10.1103/PhysRevLett.52.997).
- [10] K Kim, KD Jordan, Comparison of density functional and MP2 calculations on the water monomer and dimer, *J. Phys. Chem.* 98 (1994) 10089–10094, doi:[10.1021/j100091a024](https://doi.org/10.1021/j100091a024).
- [11] V Barone, M Cossi, Quantum calculation of molecular energies and energy gradients in solution by a conductor solvent model, *J. Phys. Chem. A* 102 (1998) 1995–2001, doi:[10.1021/jp9716997](https://doi.org/10.1021/jp9716997).